Greener Journal of Geology and Earth Sciences
ISSN: 2354-2268
Vol. 5(1), pp. 52-75, 2023

http://gjournals.org/GJGES

Characterization of the Volcano-Seismic Activity around Nyamulagira Volcano and the Location of its Crater by Means of Unified Scale

Mukange Besa Anscaire[1], Kuzituka Timothée[1], Zana Ndotoni André[1], Tondozi Kento Franck [1, 2]

[1]Mention Physics, Faculty of Sciences and Technology, University of Kinshasa, Kinshasa, DR Congo.
[2]Departement of internal Geophysics, Center of Research in Geophysic (CRG), Kinshasa, DR Congo.

ARTICLE INFO

Article No.: *120423153*
***Type*:** *Research*
Ful Text: *PDF, PHP, HTML, EPUB, MP3*

Accepted: *06/12/2023*
Published: *30/12/2023*

***Corresponding Author**
Prof. Mukange Besa Anscaire
E-mail: *anscairbesa@ yahoo.fr*

Keywords: *DRC-Virunga, Nyamulagira volcano, characterisation scale, areas-grid, modules, structure factor, seismic species, geo-seismic signature, volume density*

ABSTRACT

In the Previous works, the DRC area (10°E-35°E; 6°N-14°S) was homogeneous, but once subdivided into square sub-zones of side 5°, it was rendered heterogeneous but homogeneous in the Virunga region (25°E-30°E; 1°N-4°S°) (Mukange; 2021b). The previously homogeneous Virunga zone was made heterogeneous but homogeneous in the area around the Nyamulagira volcano (29.0°E-29.5°E; 1.2°S-1.5°S), by subdividing it into square sub-zones of dimension 1°. (Mukange; 2023a). These characterisations were made possible by the development of a model that generates seismic species by using the unified scale. The goal of this research is to characterize the 'homogeneous' region surrounding the Nyiragongo volcano, subdividing it into square sub-zones of 0.1° dimension, and to find a method for locating the crater.

To accomplish this, we developed an appropriate unified scale for characterisation on the one hand, and made the following assumptions on the other: The crater is located where the volume density of the number of volcanic earthquakes is abnormally high, while the volume density of tectonic or volcano-tectonic earthquake energy is very low.

Following the processing of earthquake data from the region from 2016 to 2021, the research revealed the following:

The seismic species identified in this area are Iab, Ibc, IIIbb, and IIIbc, as well as structure factors (ab,bb and bc).

The final degree of heterogeneity in an area is 70%, corresponding to a homogeneity of 30%.

Thus, the notion of a structure's homogeneity is dependent on the scale used to observe it, - Confirmation of hypotheses. Indeed, according to the hypotheses advanced on the one hand and field observations on the other, the crater is located at the geographical coordinates [29.2°E; 1.45°S]. Other significant outcomes were obtained, including;

There is a strong correlation between the earthquake number curve and the d-value (which characterizes the ground structure).

It has been concluded and confirmed that seismic activity in this area is dependent on the soil structure.

These findings support previous research (Mukange, 2016), which found that the seismicity of the DRC is better described (diversified) in terms of longitude (West to East) than in terms of latitude (North to South).

Moving from West to East, the shape of the structure is the same for both the DRC and the Virunga region; the latter has the opposite shape to Nyamulagira. This difference is due to the fact that the Nyiragongo area is located before (29°E) the major fracture zone (30°E) where seismic activity is very intense. But, compared to 29°, the two structures have the same shape.

.

INTRODUCTION

Our previous research (Mukange, 2016; Mukange 2021a-b) on the characterisation of seismicity in an area in general, and that of the Democratic Republic of Congo (DRC) in particular, has highlighted, on a regional study scale, the homogeneity of seismicity in the Virunga area, peculiar to Nyamulagira and Nyiragongo volcanoes.

These two volcanoes are of great interest to the scientific community and merit further investigation, particularly in terms of improving monitoring and research into techniques and modeling for possible prediction.

As a result, our research on the characterisation of the Nyiragongo volcano's surroundings will include the following objectives:

- Establish the relationship between soil structure and seismic activity in the area (modelling),
- To establish the relationship between soil structure and seismic activity in the region (modeling),
- To demonstrate that, on closer inspection, this previously shown to be homogeneous seismic activity is, in fact, somewhat heterogeneous,
- Try to locate the volcano's crater using the following assumptions:

The crater is located in an area with a high earthquake density (volume).
The crater is situated in an area with a low density (volume) of energy released by tectonic or volcano-tectonic earthquakes.
The crater is located in an area with a low density of earthquakes and energy released.

The East African Rift System is portrayed as a continental extension of the global system of lithospheric fractures that run through the middle of the Atlantic and Indian Oceans and extend into the eastern part of Africa via the Gulf of Aden and the Red Sea (Mukange, 2016; Boden et al. 1988; Bantidi, 2014a).

This fracture system is divided into two branches: the eastern branch, which runs from the Afar triangle through Ethiopia and Kenya to the northern Tanzanian divergence (Figure1); Mukange, 2013; and the western branch, which runs from the Afar triangle to the northern Tanzanian divergence.

The western branch is made up of fractures that run through the Great Lakes daisy chain, from Lake Albert (617m altitude) to Lake Edward (912m), Lake Kivu (1462m), Lake Tanganyika (780m), Lake Rukwa (782m), Lake Malawi (460m), and Mount Beira in Mozambique and South-West to Lake Kariba in Zimbabwe (Figure1). This branch thus covers the majority of the DRC's eastern provinces between latitudes 4°N and 8°S.

The East African Rifts stretch more than 6,000 kilometers from the Red Sea to the Zambezi.

The two branches join at Lake Malawi after splitting at the Aswan Lineament (Figure 1).

The DRC's seismic activity also includes the typical intra-plate fractures that affect the entire Congolese basin, known as the "Congolese craton."

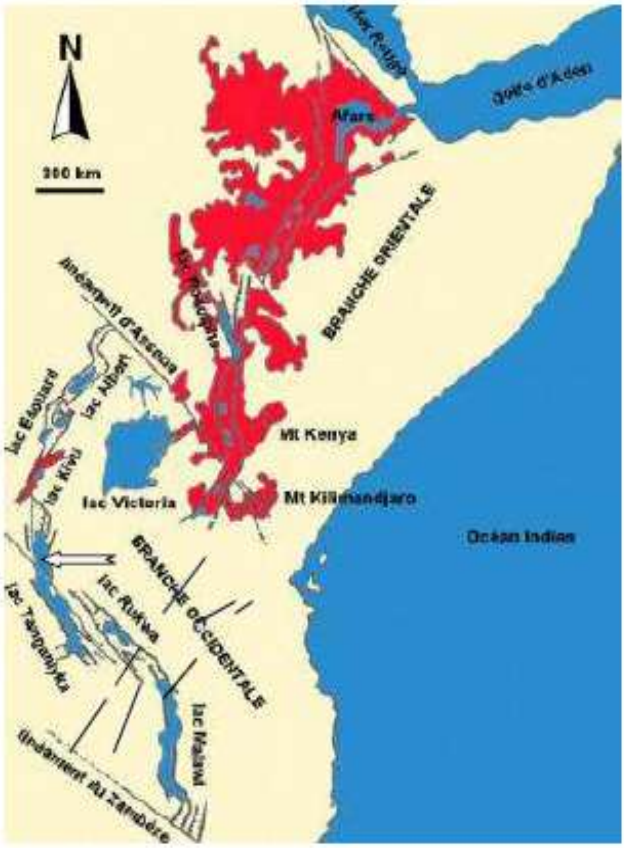

Figure 1 : East African Rift System: major faults are depicted as solid lines, while water is depicted as blue and volcanoes are depicted as red.

The Congolese Rift has three major volcanic provinces: Toro-Ankole Province in the north, Virunga Province (Nyiragongo and Nyamulagira volcanoes...) in the center, and South Kivu Province in the south (Zana and Tanaka, 1981; Zana, 1982; Ngindu, 2009). (Wafula et al., 1989; Wafula et al., 2009).

The Virunga volcanic region lies to the north of Lake Kivu. This region is made up of eight volcanoes that are divided into three groups known as volcanic provinces: the eastern group, which includes the Muhavura volcanoes (4127 m a.s.l.), Gahinga (3474 m), and Sabinyo (3647 m), and the central group, which includes the Gahinga volcanoes (3474 m) and Sabinyo (3647 m).

Central group consists of the volcanoes Isoke (3911 m), Karisimbi (4506 m), and Mikeno (4437 m), while the western group consists of Nyiragongo (3470 m) and Nyamulagira (3056 m). Except for the brief eruption of Mugogo on August 1, 1957, the volcanoes of the first two subgroups are currently dormant. Mugogo is 2350 meters above sea level and 11 kilometers north of Visoke; it is considered a satellite cone of the latter (Visoke).

Geophysical research carried out on the Virunga region in general and the Nyamulagira

volcano in particular indicate that it is characterized by a flow of feldpathic lavas (Ongendangenda, 2020).

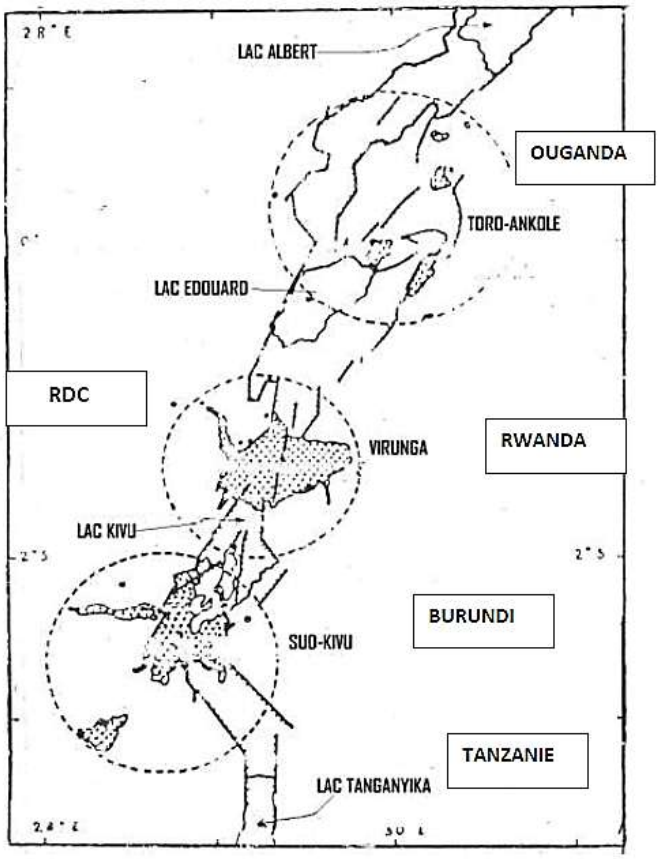

Figure 2 : The volcanic provinces of the Virunga region

The western group's volcanoes are among the most active in the world today: Nyamulagira due to the frequency of eruptions (on average every two years) and Nyiragongo due to its permanent lava lake in the central crater. It is immortant to note that Nyiragongo is regarded as one of the most dangerous volcanoes on the planet due to its proximity to the city of Goma (15 km from the crater, with an estimated population of over one million) and the superfluidity of its lava, which can flow at speeds of up to 40 km/h (Wafula, thesis). These two volcanoes are in the same area of the Rift Axis fractures (Figure 3). The volcanic rocks of these two volcanoes are basalts rich in alkaline elements with a high potassium concentration, which would explain the lava's hyper fluidity. The volcanic activity of these two volcanoes is of the Hawaiian type, characterized by effusive and passive lava emission with low viscosity (100-1000 poises) and very high temperature (1000°C). Mount Erebus in the Arctic, Kilauea in the Pacific, and Erta Alee in Ethiopia are the only other such volcanoes in the world. The frequency classification of the seismograms is similar to that of the Redoubt volcano in Alaska: type A volcanic earthquakes (4-10 Hz), type B (1-4 Hz), type C (peak at 2.6 and 8 Hz), and tremors (1-2 Hz) are recorded in the Virunga area. The last eruption of Nyiragongo volcano occurred on May 22, 2021.

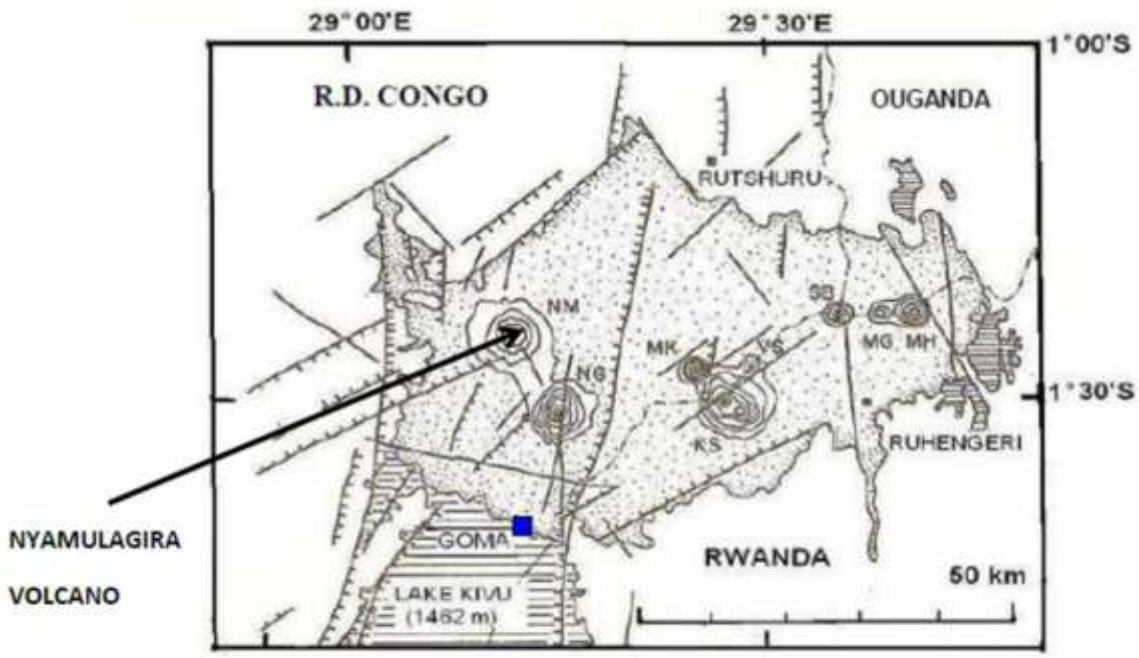

Extrait de la carte géologique de la région des Virunga.
Les lignes fermées : contour d'édifices volcaniques.
et : failles principales.
NM: volcan Nyamulagira; NG: volcan Nyiragongo; MK: volcan Mikeno;
KS: volcan Karisimbi; VS: volcan Visoke; SB : volcan Sabinyo;
MG :volcan Gahinga; MH : volcan Muhavura.

Figure 3 : Structural geology of the Virunga region and location of volcanoes

More than 1300 volcanoes provide a rhythm to the earth's internal activity. The majority of them are active.

Nyamulagira is a volcano in the Democratic Republic of the Congo (DRC) and one of the most active volcanoes in Africa. It is one of the volcanoes on the western branch of the Great Rift Valley and is part of the Virunga Mountains.

Nyamulagira volcano is bounded to the northwest by the town of Burungu, to the south-southeast by Nyiragongo volcano, to the south by Lake Kivu, and to the southwest by the town of Sake.

Nyamulagira volcano rises 3058 meters above sea level and has a summit caldera two kilometers wide by 2.3 kilometers long, surrounded by hundreds of meters high cliffs.

Slopes of Nyamulagira volcano are not very pronounced, as is typical of shield volcanoes, and give the volcano a volume of 500 km3 compared to its immediate neighbor Nyiragongo volcano.

These slopes are punctuated by fissures and scoria cones, and they are covered by basaltic lava flows with a high potassium content that are very extensive, sometimes reaching lengths of 30 kilometers.

This fissure is thought to be the main source of Nyamulagira's weakness. As a result, it is the most active zone of the Nyamulagira and Nyiragongo volcano fields.

Earthquakes at Nyamulagira volcano are caused by magma accumulation in the magma chamber. Seismographs record a plethora of micro-earthquakes (tremors) caused by fractures in compressed rocks or magma degassing.

The progressive rise of the hypocenters (linked to magma rise) indicates that the Nyamulagira volcano is in the process of awakening and that an eruption is imminent.

Because Nyamulagira is a shield volcano, the lava it produces is polygenic. This is due to the volcano's fluid and hot magmas, which allow for a two-phase conviction that prevents the chimney from closing due to material solidification.

Nyamulagira volcano is capable of dumping tens of millions of cubic meters of lava into nature in the form of flows reaching more than 20 kilometers from the point of emission, annihilating everything in its path. The volcanic products emitted, such as slag, volcanic ash, Pelee's hair, and so on, can travel a long distance with the wind, destroying and polluting fields, pastures, and river waters.

.

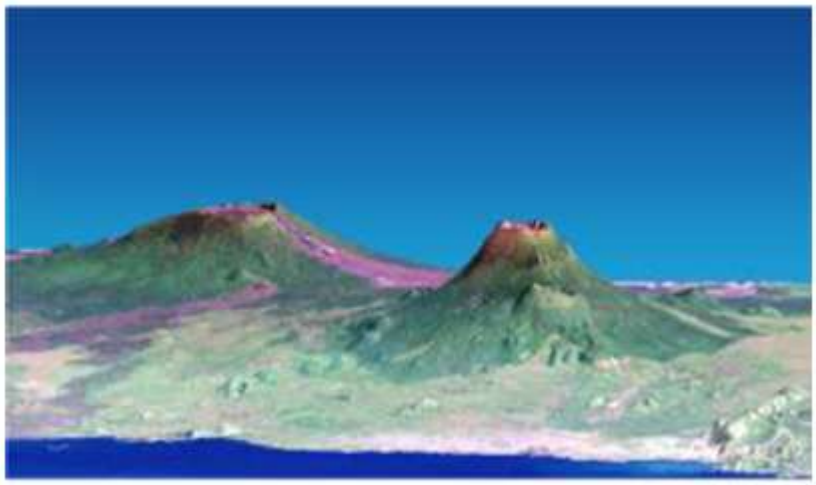

Figure 4a: Panorama of Nyamulagira volcano.

Nyamulagira volcano eruptions have wreaked havoc on the Virunga National Park, killing many animals and destroying vast swaths of land.

The plume of smoke and dust emitted during each eruption can rise into the atmosphere to the base of the stratosphere, obstructing air navigation and causing aircraft damage if pilots are not warned to avoid the affected area.

Since 1980, the Nyamulagira volcano has erupted every two years on average. Nyamulagira volcano has erupted more than 30 times on its flanks with lava flows since the turn of the century (Table 2.1). The various cones associated with the eruptions of Nyamulagira volcano have been depicted on the map (Fig. 2.10).

The most recent eruption of Nyamulagira volcano occurred on April 18, 2018.

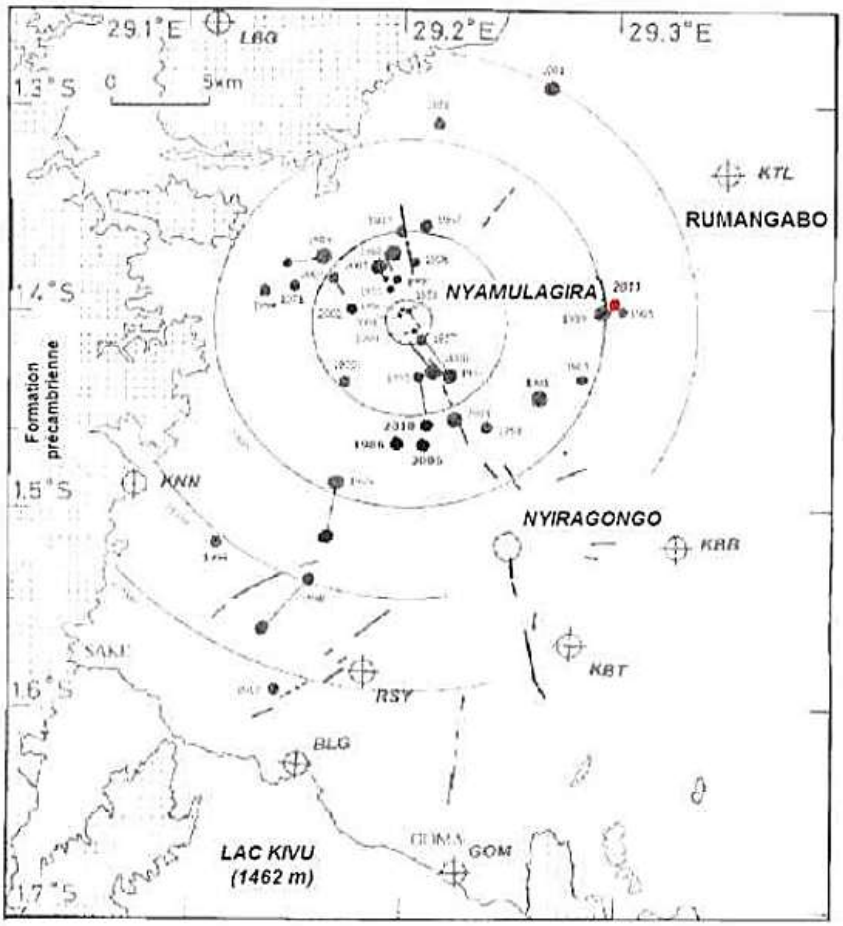

Figure 4b: depicts the distribution of the various cones associated with the eruptions of the volcano Nyamulagira from 1901 to 2011. (after Kasahara, 1991, modified).

- Eruptive sites are indicated by a solid black circle.
- Red solid circle: eruptive site from 2011.
- BLG: Bulengo, GOM: Goma, KBT: Kibati, KBB: Kibumba, KNN: Kunene, KTL: Katale, LBG: Luboga, RSY: Rusayo.

DATA ANALYSIS AND METHOD

Data analysis

The basic data for Nyamulagira volcano were collected at the Goma Volcanological Observatory (GVO) between 2016 and 2021, covering the geographical area between 29°E and 29.5°E longitude and 1.2°S and 1.5°S latitude (Figure 5). These data, however, lack magnitudes.

These data, however, lack magnitudes. In order to respond to the second hypothesis, we have associated the tectonic earthquakes with their magnitudes provided by the USGS agency.

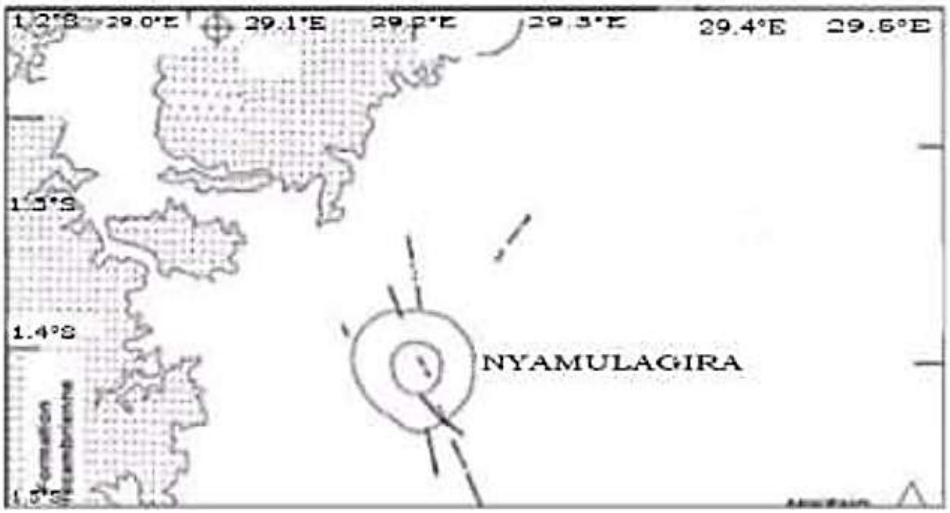

Figure 5 : Area Circumscription being investigated: Surroundings of Nyamulagira volcano

The fundamental data for each event includes the elements illustrated in the table below.

Table 1: Illustration of fundamental seismic data

Year	Month	Day	Hour	Minute	Second	Latitude	Longitude	depth (km)
2016	8	16	9	32	8,7	-1,447	29,181	4,1
2016	11	12	17	11	43,9	-1,447	29,218	5,6
2021	5	20	2	7	13,8	-1,448	28,565	17,1
2016	11	12	17	15	15,5	-1,449	29,204	23
2017	5	18	6	31	51,6	-1,453	29,104	30,8
2016	4	20	22	32	48,9	-1,453	29,156	41,5
2021	3	6	20	44	52,9	-1,457	29,327	52,7
2016	12	2	8	35	18,7	-1,462	29,267	66,9
2019	6	26	19	1	19,7	-1,464	29,27	70,4
2021	8	9	2	29	49,7	-1,465	29,173	79,8

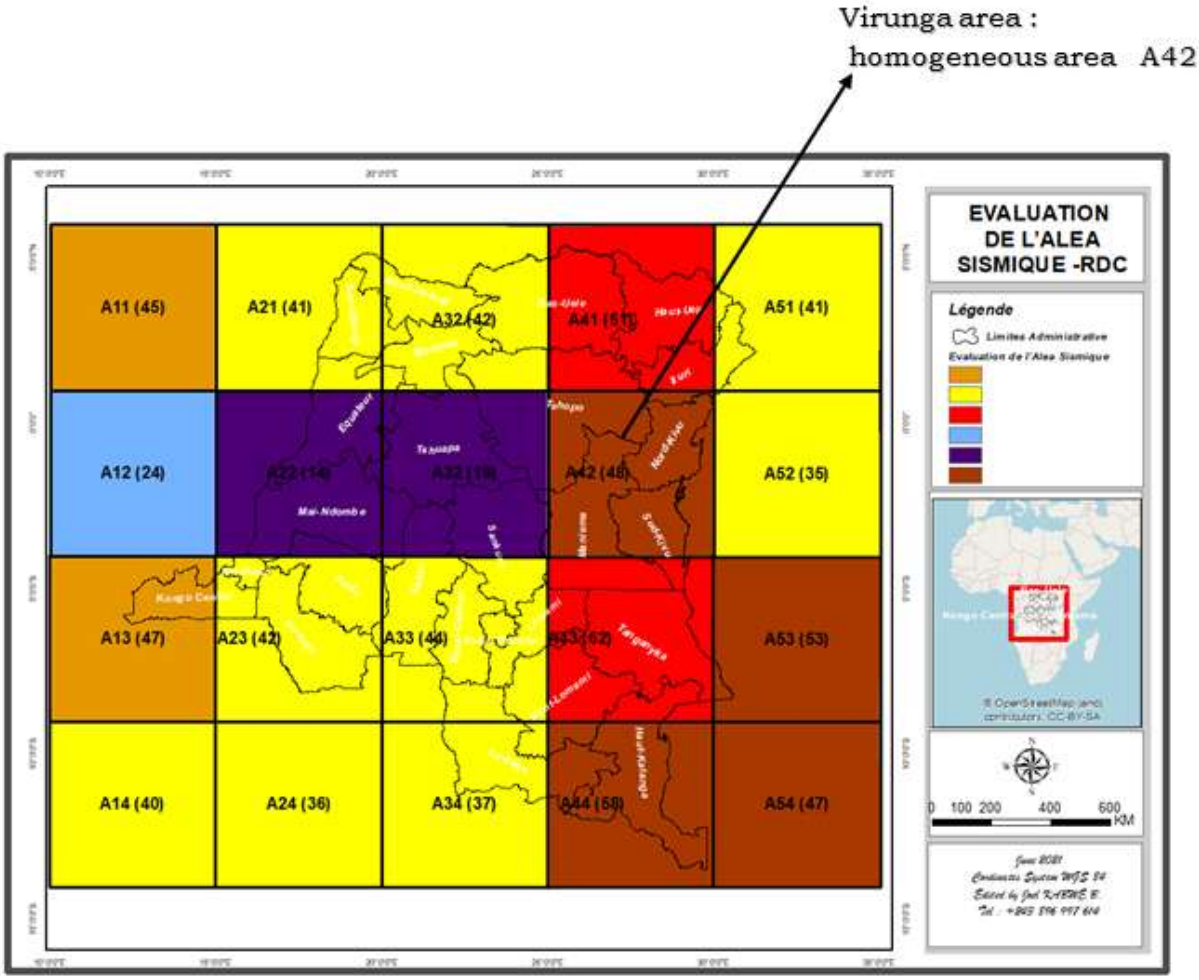

Figure 6: Seismic zoning for DRC seismic hazard assessment: seismic structure

The figure above illustrates a study area within the geographic range of 10°E-35°E longitude and 6°N-14°S latitude. The study area (29.0°E-29.5°E and 1.45°S-1.75°S) is included in the "homogeneous" seismic area A42 (25°E-30°E and 4°S-9°S).

The results of the above figure have been transformed into curves, known as "geoseismic signature" (Figure 7).

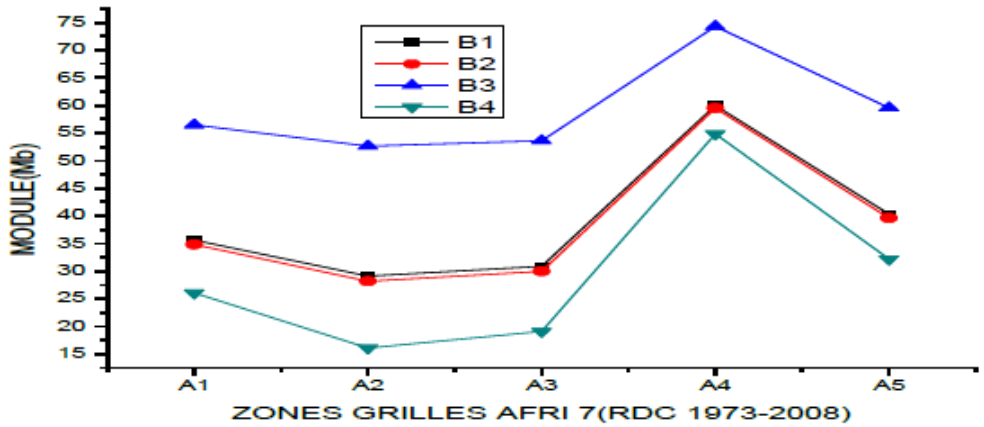

Figure 7 : Geo-seismic signature of the DRC area

A more detailed study (Mukange, 2023c) was conducted to highlight the heterogeneity of the A42 zone (25-30°E, 1°N-4°S); it was sufficient to subdivide the said zone into square sub-zones of one degree side (Figure 8).

The area is divided into two parts by the figure (8): the sub-area between 25° and 28°E and the sub-area between 28°E and 30°E. The first sub-zone, on the other hand, is divided into two parts, one between 25° and 26°E and the other between 26° and 28°E.

A study similar to the previous ones will be conducted in this zone to characterize it and highlight its 'heterogeneous' nature.

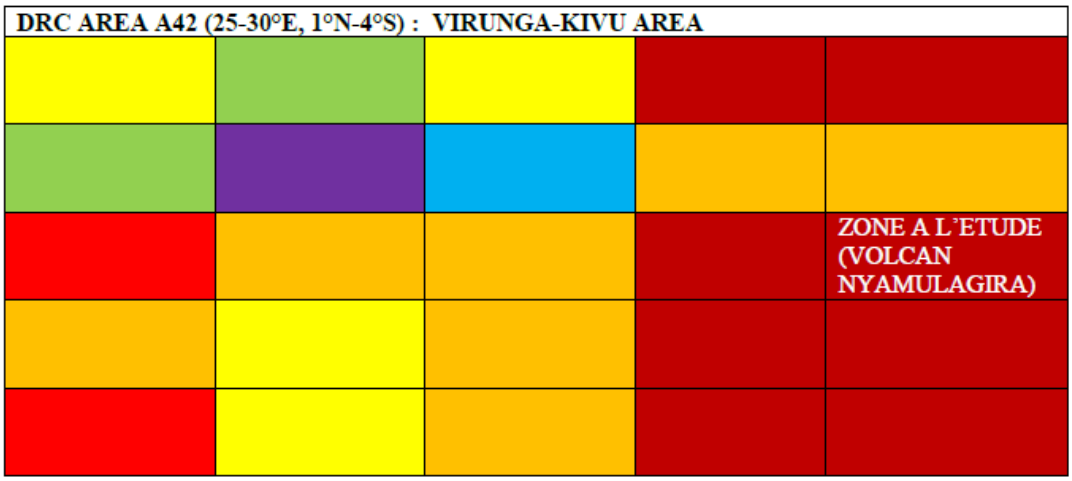

Figure 8: Seismic zoning for assessing seismic hazards in the Virunga area, A42.

The above figure's results have been transformed into curves known as "geoseismic signatures" (Figure 9).

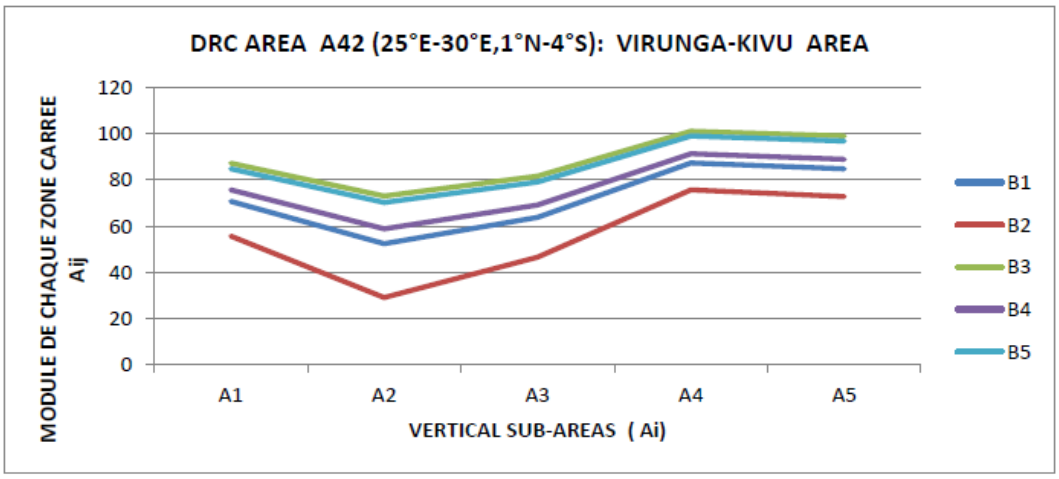

Figure 9: Geoseismic signature of the Virunga area vertical sub-areas (Ai)

The two figures below depict the distribution of hypocenters around Nyamulagira volcano.

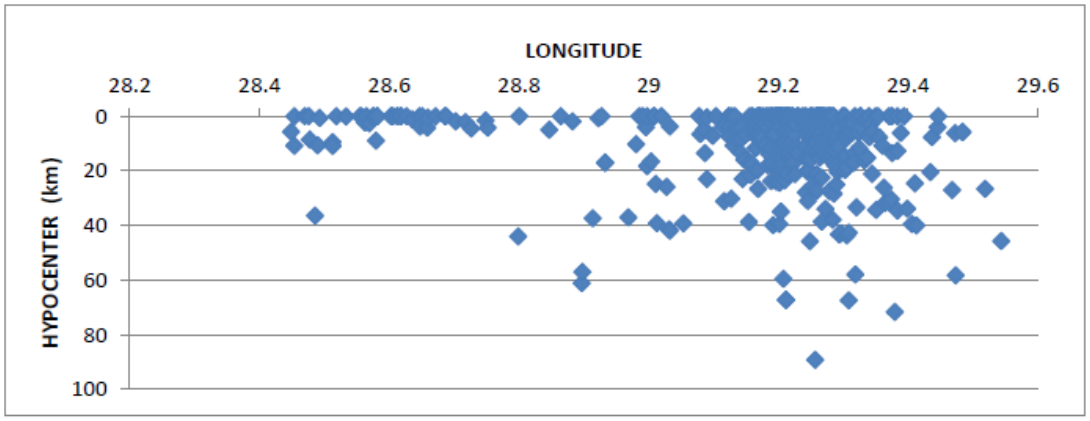

Figure 10: Distribution of hypocenters as a function of longitude around Nyamulagira volcano

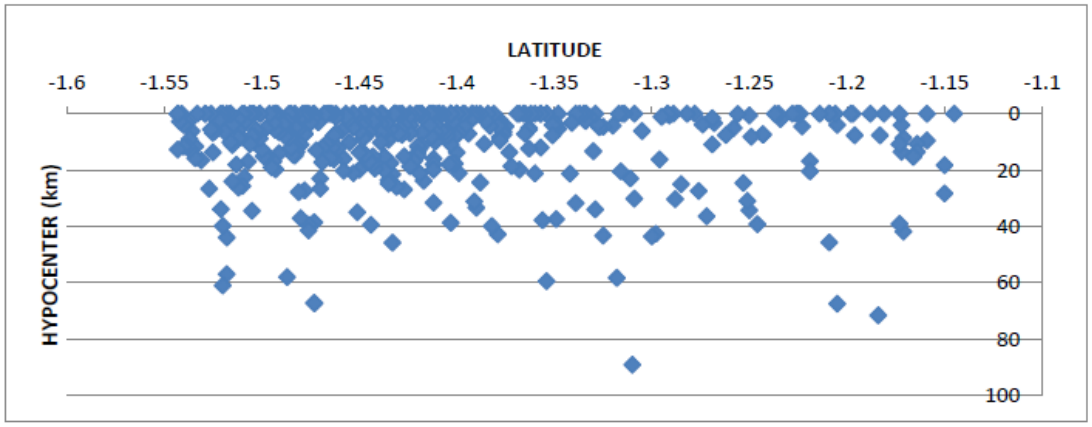

Figure 11: Distribution of hypocenters as a function of latitude around Nyiragongo volcano

2.2 Method of analysis

2.2.1. Introduction

Our primary goal is to characterize the seismicity around the volcano. To do so, we must create a unified and appropriate scale. This scale must incorporate various classical parameters that we will need to calculate in each sub-area; these parameters are as follows:

- The total number of earthquakes,
- The total energy released by earthquakes,
- The maximum Magnitude,
- The maximum depth of the hypocenters,
- Surface of each sub-area,
- Volume of each sub-area,
- The frequency of earthquakes
- Energy density,
- The b-value and "d-value" (Lay,1995; Mukange,2016)
- The degree of heterogeneity

2.2.2. Method of analysis

The data will be processed by subdividing the area into vertical and horizontal sub-areas. In each of them, we will calculate the parameters listed above and group them in a table (5).

2.2.2.1. Vertical subdivision of the area, Ai

The study area is divided into five vertical sub-areas in 0.1 degree steps from west to east (Figure 12, Table 2).

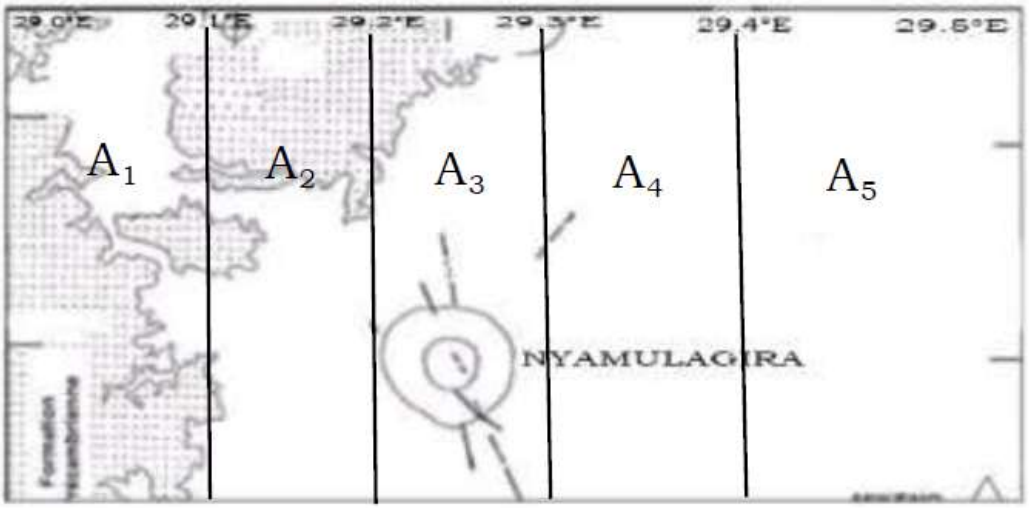

Figure 12: Subdivision of the area into vertical sub-areas (Ai)

Table 2: Limits and numbers of earthquakes in each vertical sub-area.

N°	Area	Limits of areas		Numbers of earthquakes
		Longitude(°)	Latitude(°)	
1	A1	29,0°E-29,1°E	1,2°S-1,5°S	103
2	A2	29,1°E-29,2°E	1,2°S-1,5°S	144
3	A3	29,2°E-29,3°E	1,2°S-1,5°S	146
4	A4	29,3°E-29,4°E	1,2°S-1,5°S	27
5	A5	29,4°E-29,5°E	1,2°S-1,5°S	9
Total	A1+A2+A3+A4+A5	29,0°E-29,5°E	1,2°S-1,5°S	429

2.2.2.2. Horizontal subdivision of the Bj area

The same area is, this time, subdivided into three horizontal sub-areas by steps of 0.1 degree. (Figure 13, Table 3).

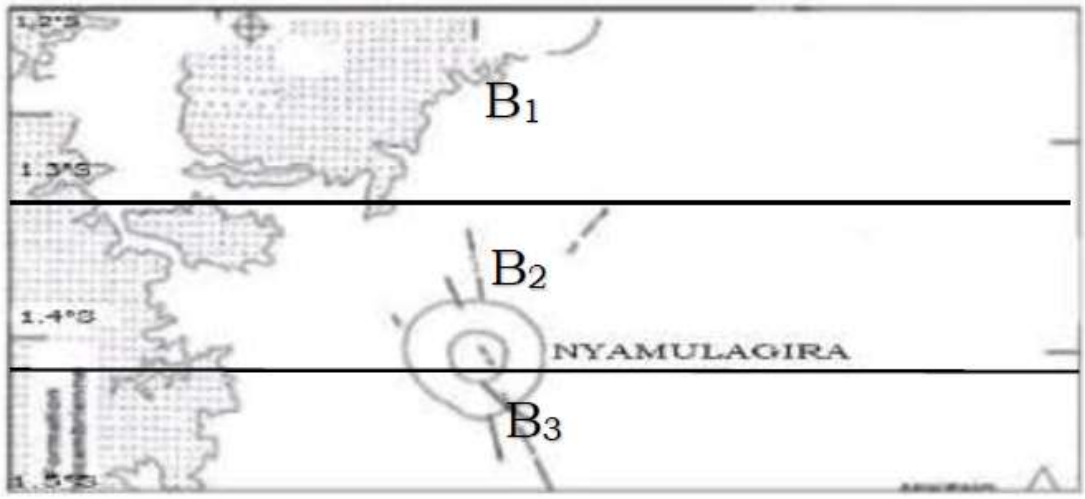

Figure 13: Subdivision of the area into horizontal sub-areas (Bj)

Table 3: Limits and number of earthquakes of each horizontal sub-area

N°	areas	Limits of areas		Numbers of earthquakes
		Longitude(°)	Latitude(°)	
1	B1	29,0°E-29,5°E	1,2°S-1,3°S	97
2	B2	29°E-29,5°E	1,3°S-1,4°S	158
3	B3	29°E-29,5°E	1,4°S-1,5°S	174
Total	B1+B2+B3	29,0°E-29,5°E	1,2°S-1,5°S	429

2.2.2.3. Calculation of Seismic Parameters

The classical seismic parameters for each sub-zone are calculated as follows:

2.2.2.3.1. The number of earthquakes

This consists of counting all the earthquakes that have occurred in each sub-area for the period from 2016 to 2021 (Tables 1-2).

These results are converted into percentages according to the following relationship:

$$N(j) = N_j.\frac{100}{N_k} \quad (1)$$

Where N_j is the total number of earthquakes in each Ai or B_j subarea N_k is the total number of earthquakes in the whole study area.

2.2.2.3.2. The maximum magnitude

The operation consists in locating the largest magnitude recorded in each sub-area.

2.2.2.3.3. The energy of the earthquakes

The seismic energy released by each earthquake is determined, in Erg, through the formula

$$logE(Erg) = 5.8 + 2.4m_b \quad (2)$$

Thus, the total energy (E_{Tk}) in the sub-zone (k) is the sum of the energies of each event.
In percent, we use the following formula:

$$E(j) = E_j.\frac{100}{E_k} \quad (3)$$

With E k, the total energy released by all recorded earthquakes in the entire study area.

2.2.2.3.4 Maximum and minimum depth

This identifies the greatest depth (hypocenter) recorded in each subarea.

2.2.2.3.5 The surface of each sub-area

Each sub-area has a rectangular shape, and its surface (S) is calculated using the following formula:

S=L.l (4)

L and l are the length and width of the subarea, respectively.
Remember that 1°=111.11km

2.2.2.3.6 The volume of each sub-area

The volume (V) of each sub-area is calculated using the following formula:

volume=area*maximum depth (5)

2.2.2.3.7. The volume density of earthquakes

The volume density (Ds) of earthquakes in each sub-area is obtained by the following formula:

$$D_s = \frac{N_s}{V} \quad (6)$$

Ns is the total number of earthquakes in each sub-zone (Ai or Bj), (V) the volume of each sub-zone.

The volume density of earthquakes in percentage is determined by the following relation:

$$D_{(sl)}(\%) = \frac{D_s.100}{D_T} \quad (7)$$

With $D_E = \frac{E}{V}$

D_T, V_T, N_T represent respectively the total density, the total volume and the total number of earthquakes of the whole area constituted by the sub-areas Ai or Bi.

2.2.2.3.8. Energy density by volume

The percentage energy density is calculated in the same way as for earthquakes, provided that the number of earthquakes in the zone or sub-zone is replaced by the energy. Hence:

$$D_E = \frac{E}{V} \quad (8)$$

In percentage it is demined for each sub-area by the following relationship:

$$D_{(Ei)} = \frac{D_{(Ei).}}{D_{(Ek)}}.100 \quad (9)$$

2.2.2.3.9. The b-value and the d-value

The relationship:

$$logE(Erg) = 5.8 + 2.4m_b \quad (10)$$

Used to characterize the seismic activity through the calculation of the value of the angular coefficient b, called the b-value (reference). This parameter has not attracted our attention. In the same way as before,
The relationship:

$$\log(N) = a' + d.H \quad (11)$$

is used to characterize the soil structure through the calculation of the value of the angular coefficient d, introduced by us, called the d-value (Table 4, Figure 14).

Where m_b is replaced by H , the depth in relation (10) .

Table 4: Statistics on the number of earthquakes by depth range

H≥	N	LOG(N)
0	103	2,01283722
5	43	1,63346846
10	36	1,5563025
15	21	1,32221929
20	19	1,2787536
25	15	1,17609126
30	12	1,07918125
35	12	1,07918125
40	9	0,95424251
45	5	0,69897
50	5	0,69897
55	2	0,30103
60	1	0

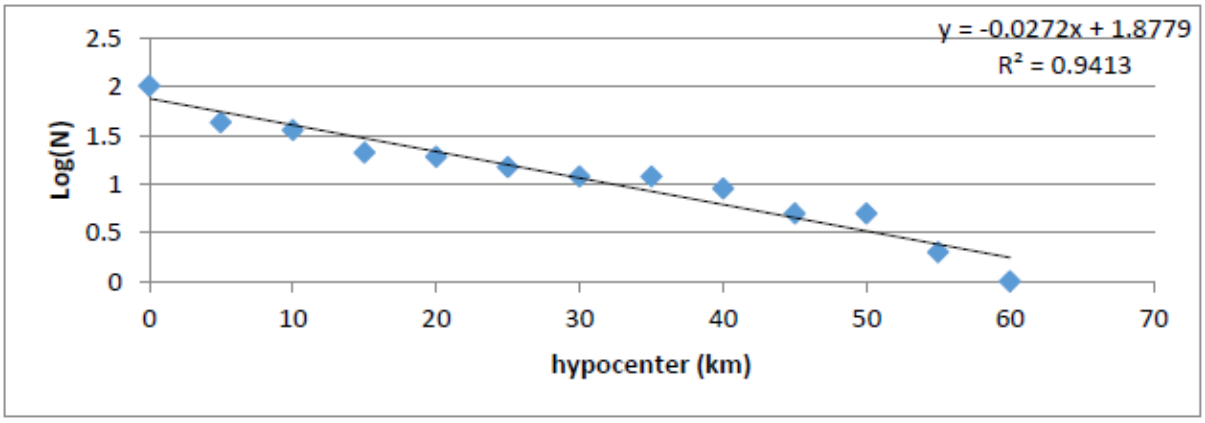

Figure 14: An illustration of how the d-value parameter is determined.

At the appropriate time, the parameter known as "degree of heterogeneity" will be defined and calculated.

3. PRESENTATION AND DISCUSSION OF THE FINDINGS

3.1. Presentation

The values of the various parameters calculated using the above formulas are shown in the table below:

Table 5: Synoptic table of calculated seismic parameters

Area	d-value	number of earthquakes	number of earthquakes (%)	Max magnitude	Energy (Erg)	Energy (%)	Hmax (km)	surface (km²)	volume (km3)	Density volume earthquakes	Density volume earthquakes	Density volume earthquakes (%)	Densityof energy (%)
A1	0,027	103	24,00932	4,24	9,68E+15	3,02E-01	61	363	22143	0,004651583	4,37E+11	175,1499866	2,20E+00
A2	0,028	144	33,56643	4,47	3,39E+16	1,06E+00	67	363	24321	0,005920809	1,39E+12	222,9412379	7,02E+00
A3	0,029	146	34,03263	4,44	2,91E+16	9,08E-01	89	363	32307	0,004519144	9,01E+11	170,1631702	4,54E+00
A4	0,03	27	6,293706	4,02	2,84E+15	8,86E-02	71	363	25773	0,001047608	1,10E+11	39,44646902	5,55E-01
A5	0,031	9	2,097902	4,91	3,85E+17	1,20E+01	58	363	21054	0,000427472	1,83E+13	16,09597299	9,21E+01
B1	0,032	97	22,61072	5,09	1,04E+18	3,24E+01	89	616	54824	0,001769298	1,90E+13	66,62087912	9,56E+01
B2	0,033	158	36,82983	5,13	1,32E+18	4,12E+01	60	616	36960	0,004274892	3,57E+13	160,9661172	1,80E+02
B3	0,034	174	40,559	4,91	3,85E+17	1,20E+01	67	616	41272	0,004215933	9,33E+12	158,7461046	4,70E+01
Total	0,035	429	100		3,21E+18	1,00E+02	89	1815	161535	0,002655771	1,98E+13	100	1,00E+02

3.2. Discussion of Results

3.2.1. Characterization scale design

The characterization of an area's seismic activity nece ssitates the development of a unified characterization scale that can reasonably incorporate all calculated p arameters (Table 5).
Our characterization scale consists of three paramete rs and is written as follows:

X 12, which is made up of two parts: the form factor a nd the structure factor: where X is the volume density of energy (D E in%) of each sub-area.
It is referred to as the "form factor."

X can have the value I, II, III, or IV, with I if D E (%) is 25%, II if D E25% D E (%) 50%, and III if D E (%) > 5 0%.

The number 1 in subscript represents the earthquake volume density (D s in%) of each subarea.
It is defined as follows:

If D s is greater than 50%, the number 1 takes the ind ex b, otherwise the index a.

Number 2 is interested in the d-
value and uses the following values:

If the d-
value is less than 0, then number 2 takes index a; if th e d-
value is greater than 0, then number 2 takes index b; and if the d-
value is greater than 0, then number 2 takes index c.

The group of numbers (1,2) in index is known as the " structure factor."

The combination of our three seismic parameters assi gns to each sub-
area a unique value called seismic species, the result s of which are shown in Table (7).

3.2.2 Interpretation of results

Interpretation of the results consists of characterizing t he area and locating the volcano's crater based on th e obtained results and hypotheses.

3.2.2.1. Seismic species, seismic levels, and color

The seismic species associated with each sub-area were ranked in ascending order based on the level of seismic activity and ground structure.

Finally, each seismic level is assigned a color (Tables 6-7).

If D s is greater than 50%, the number 1 takes the index b, otherwise the index a. Number 2 is concerned with the d-value and uses the following values: If d-value is less than 0, then number 2 takes index a; if d-value is greater than 0, then number 2 takes index b; and if d-value is greater than 0, then number 2 takes index c.

The group of numbers (1,2) in index is referred to as the "structure factor."
The combination of our three seismic parameters gives each sub-area a unique value called seismic species, the results of which are shown in Table (7).

Table 6: Each seismic level is assigned a color

Seismic level	colour
1	Rose
2	bleu
3	Vert
4	jaune
5	violet
6	Orange
7	Rouge clair
8	Rouge foncé

Table 7 : Each subzone has a different color code, seismic species, and seismic level.

Sub areas	Seismic species	Seismic level$(a_i)\ ou\ (b_j)$	Colour code
A1	IIIbc	7	Light red
A2	Ibc	4	Yellow
A3	Ibc	4	Yellow
A4	Iab	1	Pink
A5	Iab	1	Pink
B1	IIIbb	6	Orange
B2	Ibc	4	Yellow
B3	IIIbc	7	Light

Because of the reason, this scale differs from previous ones (MUKANGE 2021a) in a few ways: With several parameters,

• She has been greatly simplified to fit into three parameters; • She incorporates the structure constant known as the d-value;

• She introduces the concept of volume density (of energy or a number of séisms).

3.2.2.2. Vertical and horizontal zone map

The results of Table (7) are used to create the seismic zone maps shown below.

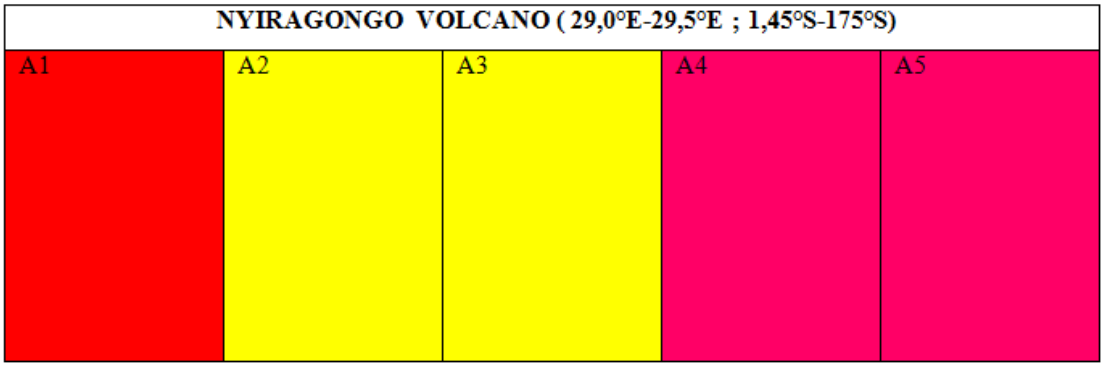

Figure 15: Seismic zoning map, vertical subdivision.

As we can see on the map below, the sub-zones A2 and A3, A4 and A5 have the same structure. A1 has a unique, high structure.

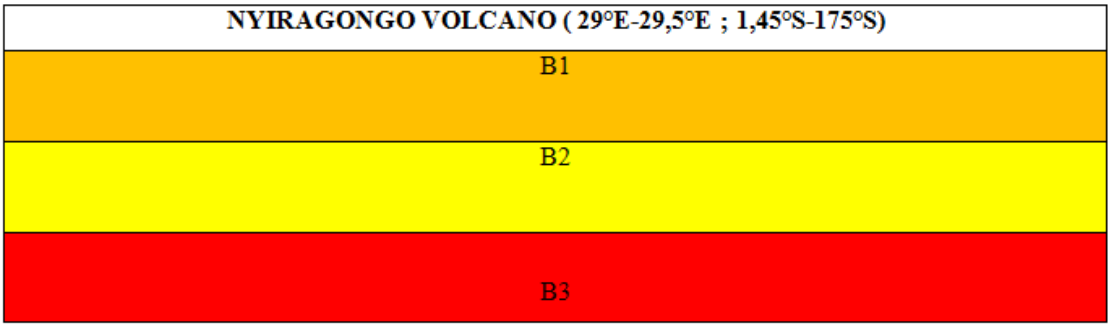

Figure 16: Seismic zoning map, horizontal subdivision.

We notice that each sub-area is distinct, and that when comparing the two subdivisions (Figure 15 and 16) on the eight sub-areas, two colors are shared (yellow and red). This demonstrates that seismicity and ground structure are not the same when studied vertically or horizontally.

3.2.2.3 Degree of heterogeneity

The degree of heterogeneity is determined by the ratio (in percentage) of the number of different colors to the total number of sub-zones (Table 8). It can also be calculated as the ratio of the distinct colors to the total number (8) of possible colors in the table (7).

Table 8 : shows the overall degree of heterogeneity of the sub-areas.

Sub-areas	Degree of heterogeneity	Degree of heterogeneity in %
A_i	3/5	60 %
B_j	3/3	100 %
Average		80%

We note that this area, which was previously homogeneous and subdivided into sub-areas, is no longer homogeneous: when studied vertically and horizontally, it exhibits a degree of heterogeneity of 60 and 100%, respectively, for an average of 80%.

3.2.2.4 Interpretation of other parameters

The evolution of the parameters according to sub-areas is shown below.

3.2.2.4.1 D-value evolution

The d-value defines the soil structure, and its evolution by sub-area is as follows:

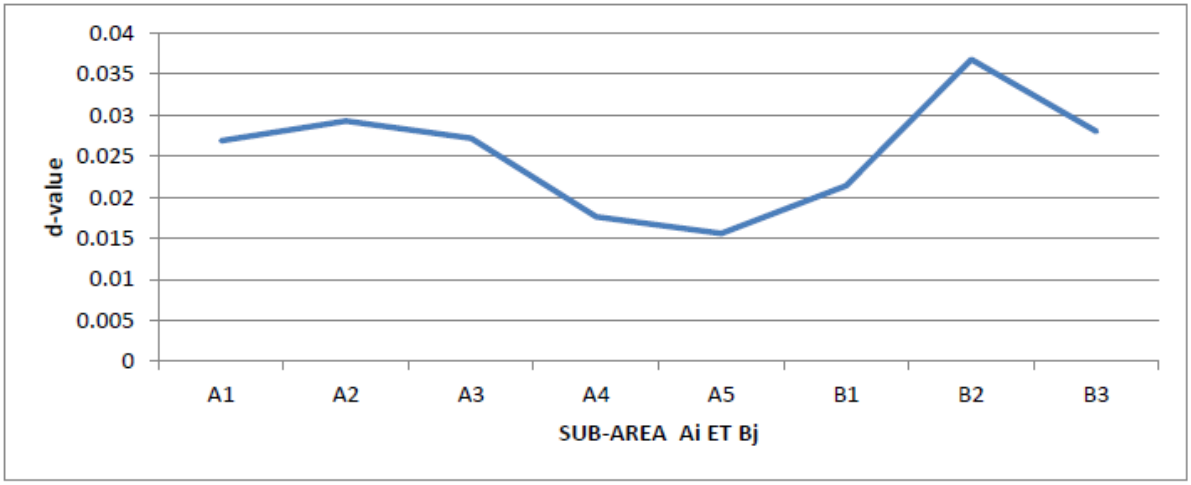

Figure 17 depicts the evolution of the parameter d-value in each sub-area.

This curve demonstrates that the structure of the sub-area A2 is similar to that of A4 and the same as that of A3 and A5.

3.2.2.4.2 The evolution of Ai and Bj as a function of maximum depth

The characterization is carried out here by following the distribution of hypocenters on each vertical sub-area.

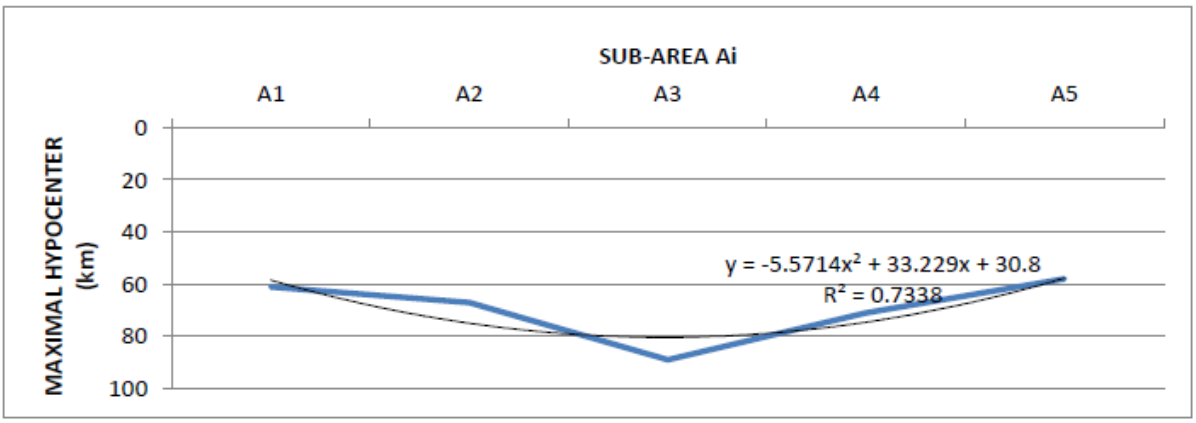

Figure 18: Distribution of maximum hypocenters in each Bj sub-area: modeling

We observe that the distribution of maximum hypocenters from West (A1) to East (A5) around Nyamulagira volcano follows a parabolic law of upward concavity;

The shape of the above curve is similar to that obtained in our previous research (Mukange, 2021b).

Indeed, the curve below shows the seismic activity (modulus on the ordinate) as a function of depth in the basaltic (Bi, on the abscissa) and sub-basaltic (SM1) layers in the Virunga area, i.e. from 25 to 105 km depth.

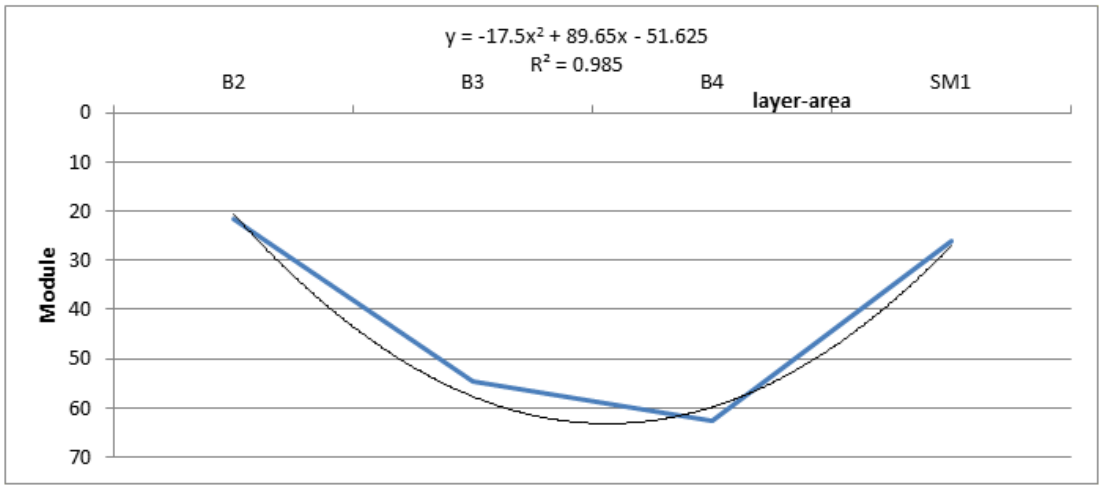

Figure 19: Seismic activity behavior in the basaltic and sub-basaltic zone of the Virunga area

We conclude that the ground structure studied in the area of the volcano going from west to east (vertical subdivision, Ai) is similar to that studied, in terms of seismic activity, in the Virunga region at a depth of between 25 and 105 km (Figure 19). These two parabolic curves are the inverse of the one that describes the seismic structure studied in the vicinity of the volcano going from North to South (Figure 20).

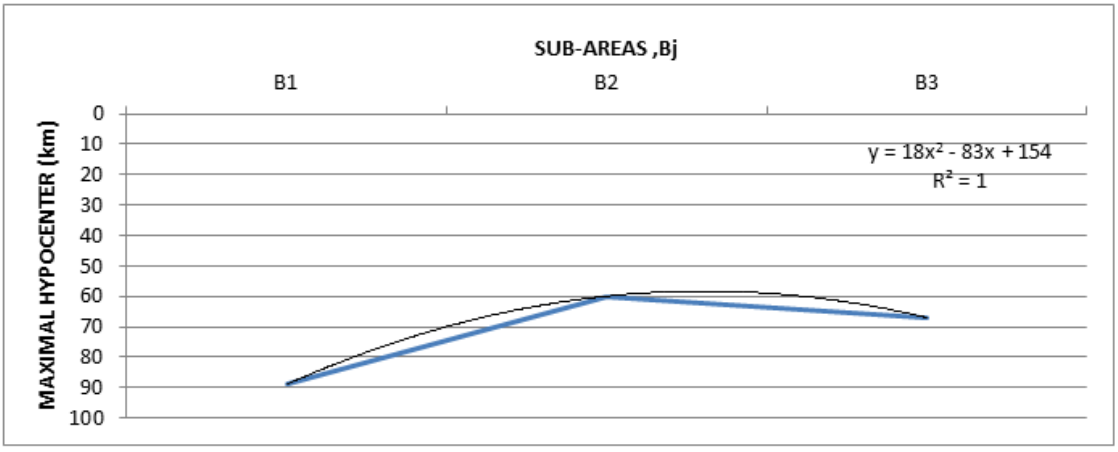

Figure 20: Distribution of maximum hypocenters in each Bj sub-area of the volcano region: modeling.

The above curve has a similar shape to that obtained in our previous research (Figure 21).

Indeed, the curve below depicts seismic activity (modulus on the ordinate) as a function of depth in the Virunga region's granitic layer (Gi), i.e. from 0 to 20 km depth.

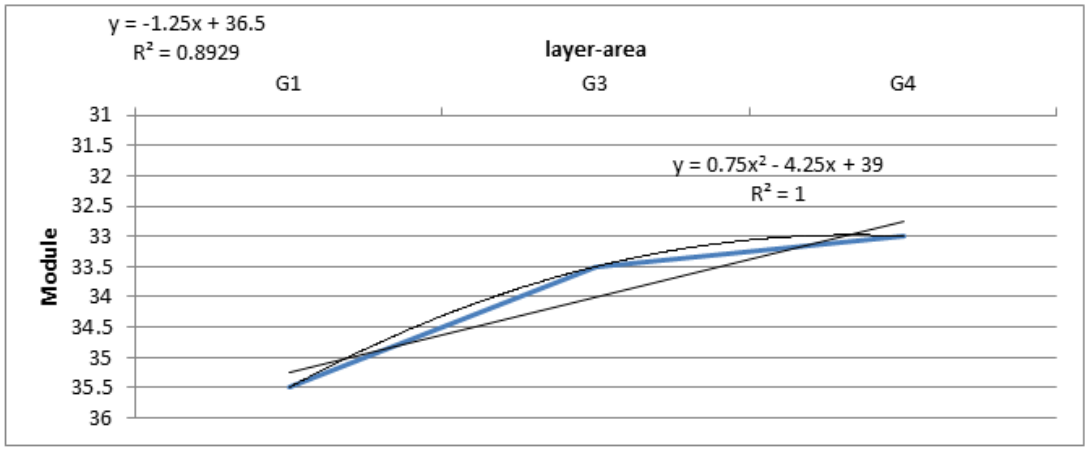

Figure 21: Seismic activity behavior in the granitic zone (0-20 km) of the Virunga area.

3.2.2.4.3. Comparison between soil structure and seismic activity

The following curves, Figure 22 and 23, present respectively, through their angular coefficients (b-value and d-value), the seismic activity and the ground structure in the Virunga area.

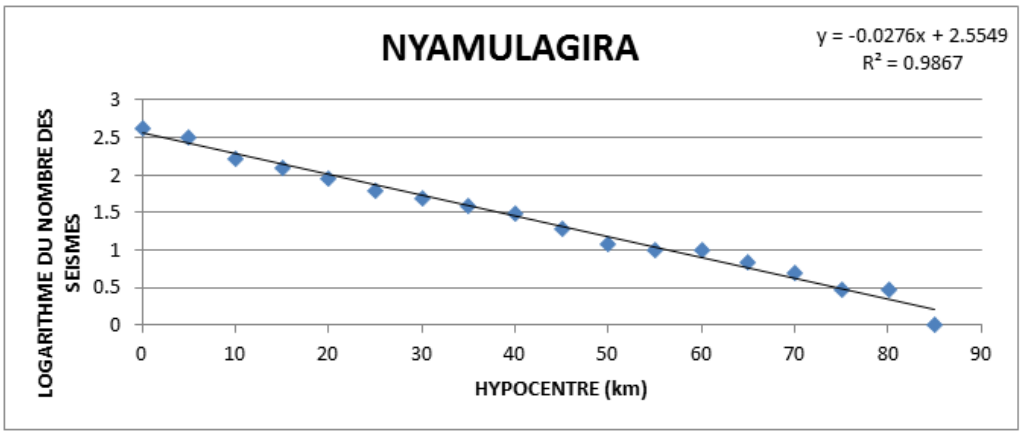

Figure 22: Model of the ground structure around Nyamulagira

According to this model, the number of earthquakes decreases inversely as depth increases. The same is true for the number of earthquakes in relation to their magnitude (Figure 23).

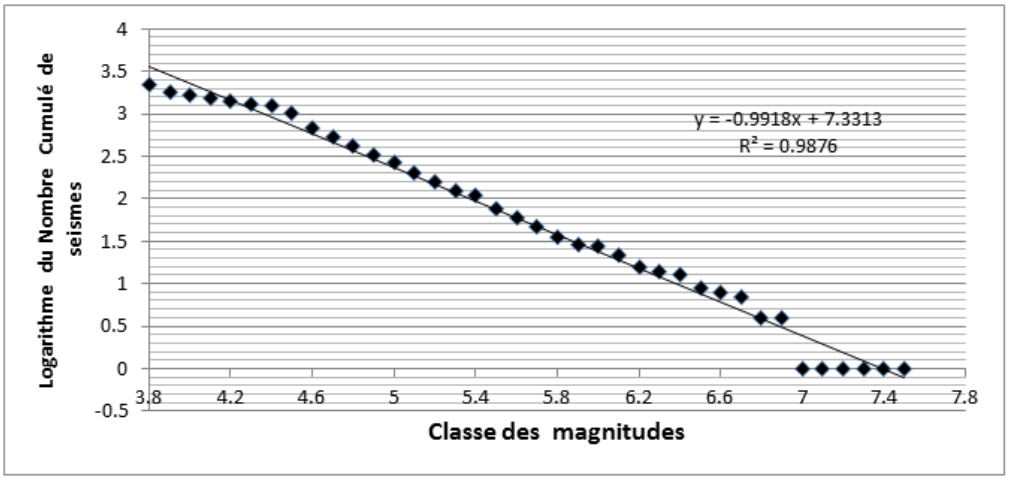

Figure 23: Model of seismic activity in the Democratic Republic of Congo

Because these curves appear to have the same tendency (negative slopes and almost parallel), there is reason to believe that there is a linear relationship between soil structure and seismic activity.

3.2.2.4.4. Distribution of seismic energy and number of earthquakes by sub-area

The curve below depicts how earthquakes and energy are distributed in each sub-area.

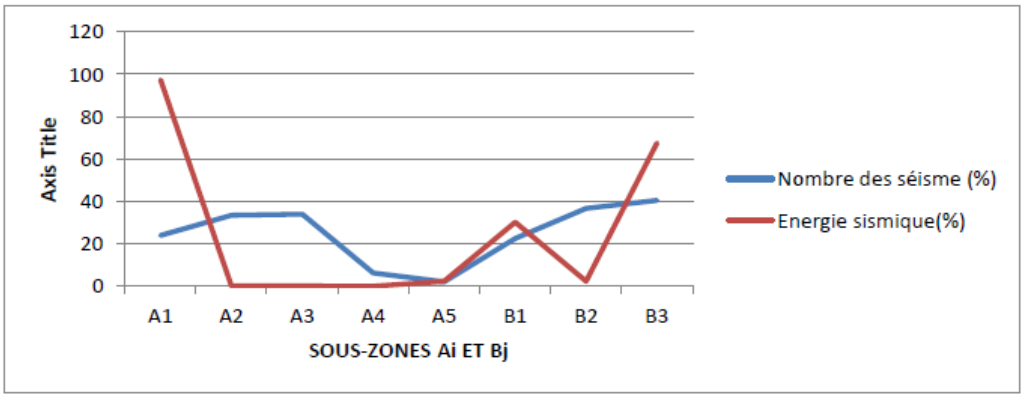

Figure 24: Distribution of seismic energy and number of earthquakes by sub-area.

It is worth noting (Figure 24) the following:

- As a function of Ai and Bi, the number of earthquakes increases at A3 and B3, respectively.
- According to Ai and Bi, the energy released is greater in A1 and B3, respectively.
- According to Ai and Bi, the number of earthquakes is lower at A5 and B1, respectively.
- As a function of Ai and Bi, the released energy is lower at (A2, A3, and A4) and B2, respectively.
- No link has been found between maximum (minimum) energy and the number of earthquakes.

The curve below depicts the distribution of earthquake density and energy in each sub-area.

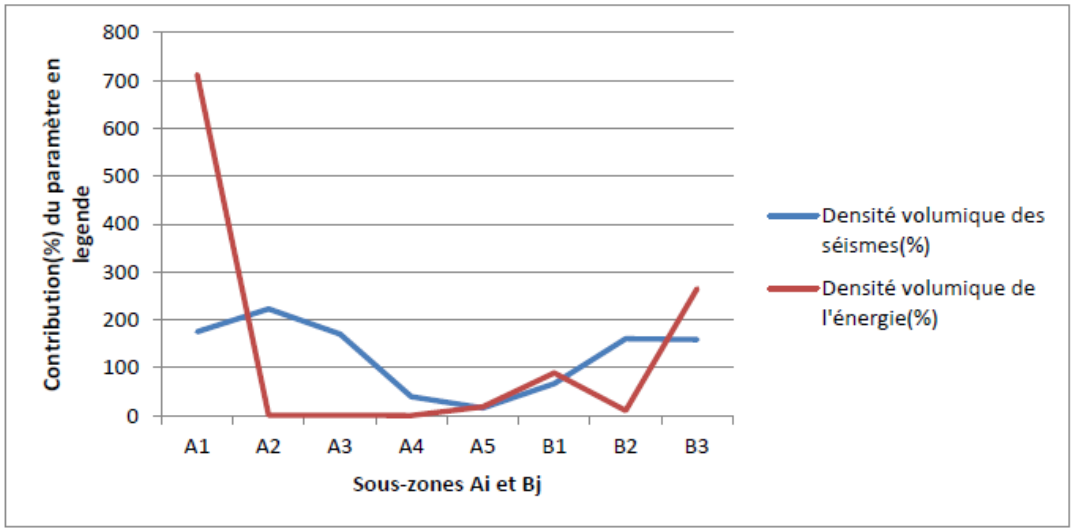

Figure 25: Distribution of seismic energy density and earthquakes by sub-area

The above figure shows the following:

- As a function of Ai and Bi, the volume density of the number of earthquakes is higher at A2 and B2 respectively,
- As a function of Ai and Bi, the volume density of energy released is higher at A1 and B3 respectively,
- As a function of Ai and Bi, the volume density of the number of earthquakes is lower at A5 and B1 respectively,
- As a function of Ai and Bi, the volume density of the released energy is lower at A2 and B2 respectively,
- With a few exceptions, there is a correlation between the minimum energy density and the maximum density of earthquakes at the same location, and vice versa. This is consistent with the assumptions made,
- The assumptions made at the start have been validated at sub-areas A2 and B2, the most likely location of the crater.

It is concluded that the characterization of seismicity should be described in terms of volume density rather than number of earthquakes or energy. Thus, the concept of volume density is crucial in this study and in the field of characterization in general.

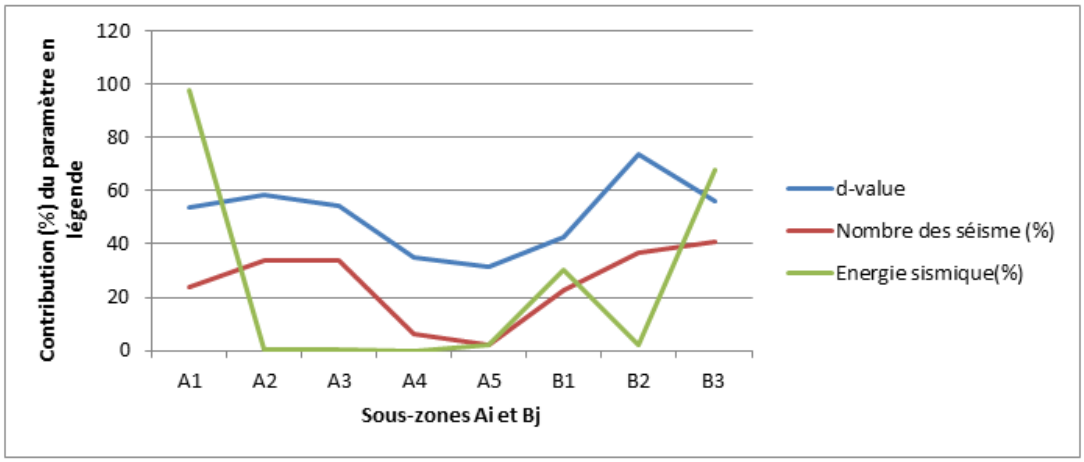

Figure 26: Distribution of energy, number of earthquakes and d-value by sub-zone
NB: the value of the d-value has been multiplied by 2000

Once again, a good correlation is observed between the curve of the number of earthquakes and the d-value (which characterizes the structure of the ground). We conclude and confirm that the seismic activity depends on the structure of the ground.

3.2.3. Division of the studied area into grid-areas (Cij) and calculation of the degree of heterogeneity.

The concept of grid-areas is related to that of the vector representation (Mukange, 2016)
Indeed, the grid-area Cij is an intersection between the sub-areas Ai and Bj.

Thus Cij is described as follows:

i takes the seismic level values (ai) of the vertical sub-areas (Ai) ;

j takes the seismic level values (bj) of the horizontal sub-areas (Bj).

The relation $c = \sqrt{a_i^2 + b_j^2}$ (12)

allows us to calculate the modulus of the sub-areas C_{ij}. To each modulus, in accordance with the code of table (9), we associate a color to each module (Table 10).

Table 9: Color code for the module slice

MODULE	Level	Colours
$[1,2]$	1	Pink
$]3,4]$	2	Light blue
$]5,6]$	3	Purple
$]7,8]$	4	Green
$]9,10]$	5	Yellow
$]11,12]$	6	Orange
$]13,14]$	7	Light red

Table 10: Assignment of the color to the module of each zone-grid cij

GRID-AREA Cij	b	a	MODULE	SEISMIC LEVEL	COLOR CODE
C11	6	7	9	5	Yellow
C12	6	4	7	4	Green
C13	6	4	7	4	Green
C14	6	1	6	3	Purple
C15	6	1	6	3	Purple
C21	4	7	8	4	Green
C22	4	4	6	3	Purple
C23	4	4	6	3	Purple
C24	4	1	4	2	Light blue
C25	4	1	4	2	Light blue
C31	7	7	10	5	Yellow
C32	7	4	8	4	Green
C33	7	4	8	4	Green
C34	7	1	7	4	Green
C35	7	1	7	4	Green

The results of the above table, particularly the use of the color code, leads to the characterization of the grid-zones in the form of seismic zoning (Figure 27), thus highlighting four groups (Table 11):

Table 11: Statistics on the colors (module)

N°	COLOUR	AREA-GRIDS	CONTRIBUTION(%)
1	PURPLE	C14,C15,C22,C23	4/15 (27%)
2	BLUE	C24,C25	2/15 (13,3%)
3	GREEN	C12,C13,C21,C32,C33,C34,C35	7/15 (47%)
4	YELLOW	C11,C31	2/15 (13,3%)

The results of this table are converted into curves (Figure 27).

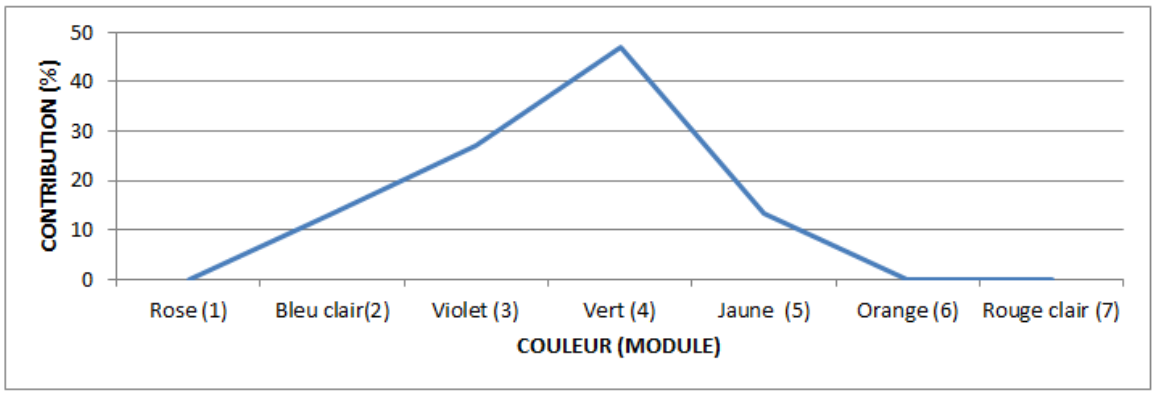

Figure 27: Distribution of colors (module) in the Nyamulagira grid zones

Based on this grouping, we estimate the degree of homogeneity to be 27% (4 groups out of 15 Cij), or a degree of heterogeneity of 73%.

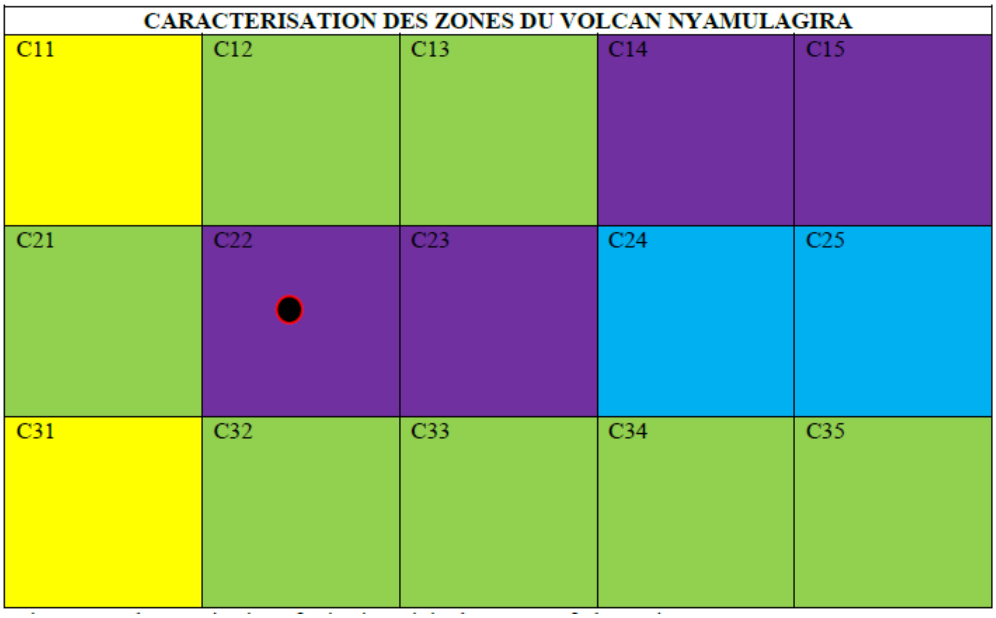

Figure 28: Characterization of seismic activity by means of the zoning map

The results of the table are transformed into curves (Figure 29) and indicate the following:

- Seismic activity decreases from the West (A1) to the East (A5),
- The B1 sub-area is the transition area between B2 (low activity) and B3 (high seismic activity).

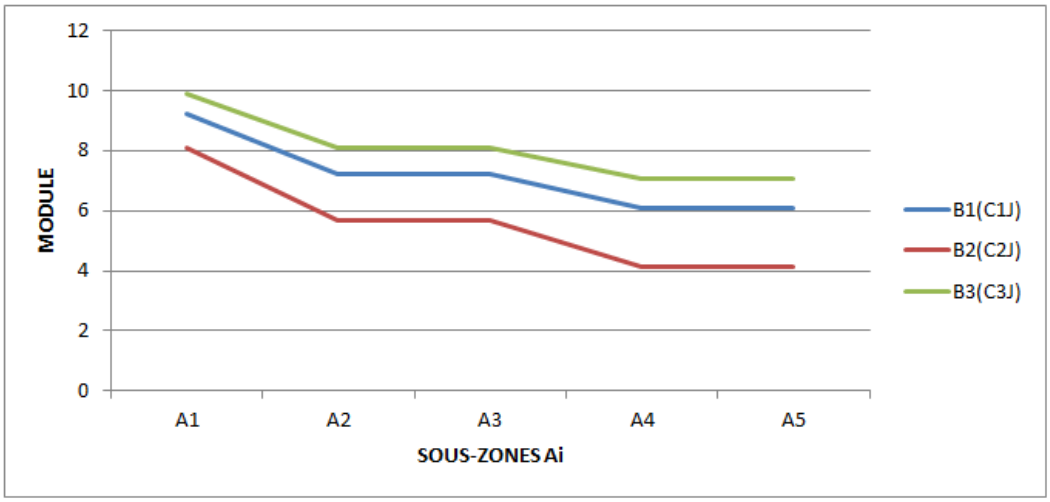

Figure 29: Characterization of seismicity using curves: structure

The diagram above reveals some intriguing anomalies:

- From West (A1) to East, the modulus decreases (A5),
- It decreases from North (B1) to South (B3),
- The shift at A4 and A5 between curves B2 and B3 is twice as large as the shift between B1 and B2; it appears that the crater is unlikely to be located at A4 or A5.
- A4 and A5 are more likely to be the site of tectonic or volcano-tectonic earthquakes than volcanic earthquakes.

Based on an analysis of the parameters that prevailed in the design of the characterization scale (including the introduction of the parameter "volume density") and seismo-volcanic activity concepts, there is a high probability that the crater is located near (A1, A2, A3) and (B1). Finally, the degree of heterogeneity is calculated as follows:

For the horizontal sub-areas (Bj), we calculate the ratio between the number of different colors recorded to the total number of Cij (five in total for each Bj), converted into percentage. For the vertical sub-areas (Ai), we calculate the ratio between the number of different colors registered to the total number of Cij (three in total for each Ai), converted in percentage,

Table 12: Degree of heterogeneity for each sub-area

Sub-areas	Degree of heterogenéity	Degree of heterogeneity in %
B_1	3/5	60 %
B_2	3/5	60 %
B_3	2/5	40 %
A_1	2/3	67 %
A_2	2/3	67 %
A_3	2/3	67 %
A_4	3/3	100 %
A_5	3/3	100 %
Average		561/800 =70%

Once zero, the degree of heterogeneity is now 70.

According to the formula, the rate of heterogeneity é is 44% (4/9) when the number of distinct colors (5) in the figure (28) is multiplied by the total number of colors in the table (9)

According to the formula number of distinct colors (4) in figure (28) on total number of boxes (15) in figure (28), the rate of heterogeneity é is worth 27% (4/15). We will stick with the first formula.

3.2.4. Comparison of the structural curves

Three structural curves are presented below.

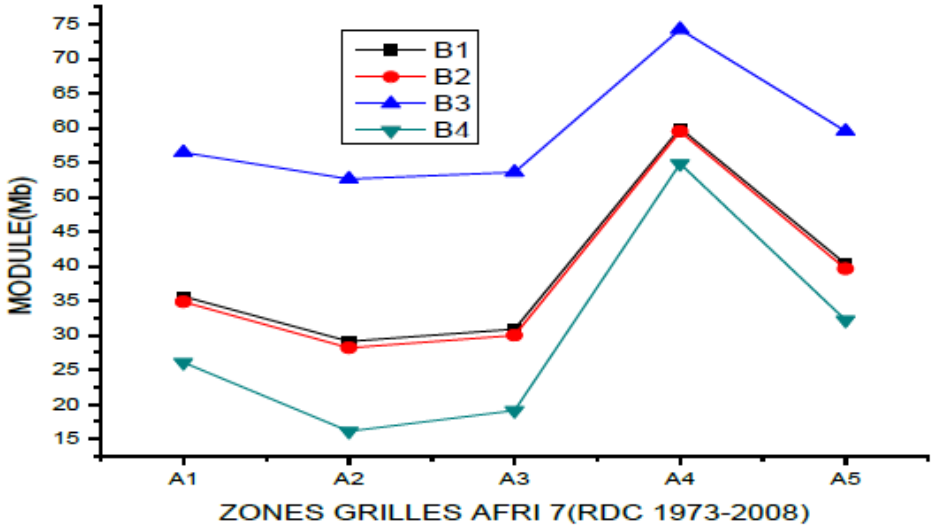

Figure 30: Geoseismic signature of the DRC (10°E-35°E; 6°N-14°S).

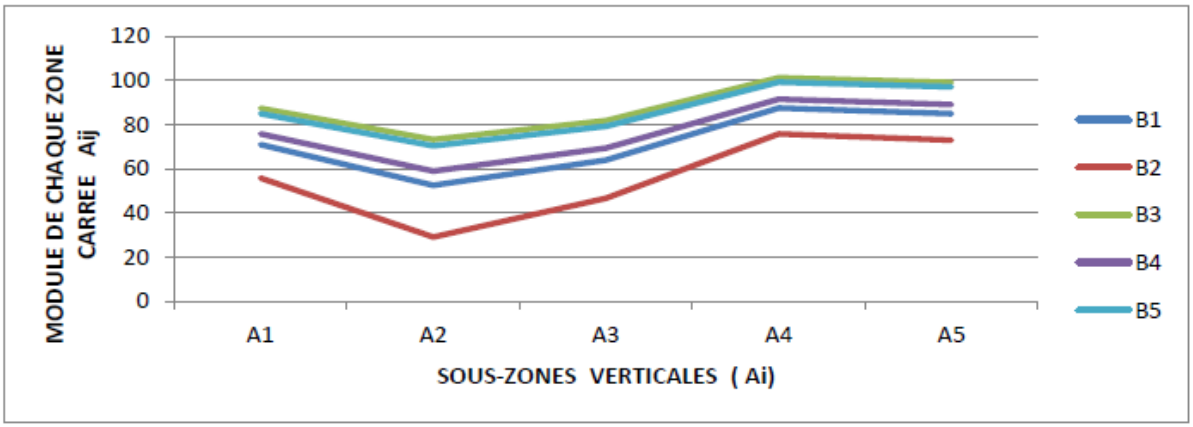

Figure 31: Geoseismic signature of the Virunga area (25°E-30°E; 1°N-4°S)

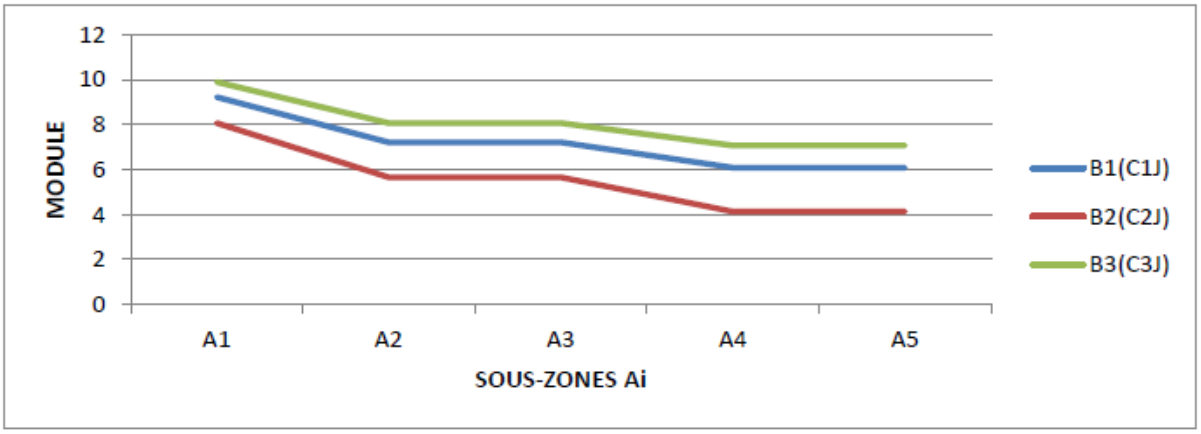

Figure 32: Geoseismic signature of the Nyamulagira Volcano area (29.0°E-29.5°E; 1.2°S-1.5°S).

Analysis of these three structures reveals the following:

Moving from west to East (Ai), the shape of the DRC (Figure 30) and the Virunga area (Figure 31) is the same; they are the inverse of the Nyamulagira (Figure 321). This difference is due to the fact that Nyamulagira area is located in the front (29°E), a less seismic zone, whereas the area of major fractures and intense seismic activity is located between 30°E and 35°E.

The three structures follow the same pattern from North to South (Bj): Seismic activity decreases from North to South.

These findings support previous research (Mukange, 2016), which found that the DRC's seismicity is better described (diversified) in terms of longitude (West to East) than latitude (North to South).

3.2.5. Crater location

Starting with the assumption that the crater is located where: - the volume density of the number is abnormally high, - the volume density of the seismic energy of tectonic or volcano-tectonic earthquakes is very low.

Based on these assumptions, the other distinguishing features discussed above, and the results in Figures (24-25), the crater is located at C22 (B2, A2) [29.15°E; 1.35° S], as indicated by the black bubble in Figure (28). These findings are consistent with the observations made in the field (Figure 5). This confirms our stated hypotheses, which must generalize and be confirmed further through additional research.

4. GENERAL CONCLUSION AND PERSPECTIVES

The design of a characterization scale enabled the study of volcano-seismic activity in the vicinity of Nyamulagira volcano in the DRC's Virunga area, the western branch of the East African Rifts, as well as the search for techniques for locating its crater on the basis of seismic data. This scale,,, very simplified because it contained only three parameters, introducing the structure constant known as the d-value and the concept of the volume density of energy or number of earthquakes provided the following results:

This previously homogeneous area has been subdivided into sub-areas and is no longer homogeneous: It has a degree of heterogeneity of 60 and 100%, or an average of 80%, when studied vertically and horizontally.

The area's final degree of heterogeneity is 70%, corresponding to a homogeneity of 30%. Thus, the notion of structure homogeneity is dependent on the scale used to observe it.

The seismic species identified in this area are Iab, Ibc, IIIbb, and IIIbc, with structural factors (ab, bb, and bc) identified.

Analysis of these three structures in the Democratic Republic of Congo (10°E-35°E; 6°N-14°S), the Virunga area (25°E-30°E; 1°N-4°S°), and the area around Nyiragongo volcano (29.00°E-29.50°E; 1.45°S-1.75°S) reveals the following:

Going from West to East (Ai), the shape of the structures for the Democratic Republic of Congo and Virunga is the same; they are the inverse of Nyamulagira. Nyiragongo area is located in the front (29°E), which is a less seismic zone, whereas the area of major fractures and intense seismic activity is located between 30°E and 35°E. Around 28°E, Virunga and Nyiragongo structures have the same shape.

From North to South (Bj), the three structures follow the same pattern: seismic activity decreases from North to South.

These findings support previous research (Mukange thesis), which found that the seismicity of the Democratic Republic of Congo is better described (diversified) in terms of longitude (West to East) than in terms of latitude (North to South);

- The ground structure around the volcano from north to south (horizontal subdivision) is similar to that studied in the Virunga area at a depth ranging from 25 to 105 km.
- The ground structure studied from west to east (vertical subdivision, Ai) is similar to that studied in terms of seismic activity in the Virunga area at a depth ranging from 25 to 105 km (Figure 19). These two parabolic curves are the inverse of the one that describes the seismic structure studied in the volcano's vicinity from north to south (Bj).
- We find a strong relationship between the number of earthquakes and the d-value curve (characterizes the structure of the ground). We conclude and confirm that seismic activity is determined by the ground structure.
- There is a relationship between low energy and the number of earthquakes, with some exceptions.

REFERENCES

1. Bantidi M., Wafula M., Mavambou, Mukange B., Zana Nd., (2014a). Probabilistic assessment of seismic hazard in Lake Tanganyika Rift accounting for local geologies conditions. 2015. *International Journal of Geology, Agriculture and Environmental Sciences*. Vol.03 Issue 02 (April 2015), pp24-29.

2. Bantidi M., Mukange B., et Zana N., (2014b). Structure de la sismicité de la Branche occidentale des Rifts Valleys du système des Rifts Est-africains ; de 1954 à 2010, *International Journal of Innovation and Applied Studies*, ISSN 2028-9324 Vol. 9 No. 4 Dec. 2014, pp.1562-1581.

3. Borden J-P., (1988). *Biologie-Géologie*. Première S. Paris: Bordas

4. Lay T., Wallace T., (1995). *Modern Global seismology*. New-York : Academic Press

5. Mavonga Tuluka G., (2009).*Seismic hazard assessment and volcanogenic seismicity for the Democratic Republic of Congo and surrounding areas, western Rift valley of Africa*. Thèse de Doctorat: University of the Witwatersrand (Johannesburg), Faculty of Sciences.

6. Mukange B., Bantidi M., Zana Nd., (2013). Structure de la sismicité de la Branche orientale des Rifts Valleys du système des Rifts Est-africains ; de 1954 à 2010. *Revue Congolaise des Sciences Nucléaires.* vol.27, pp 151-169.

7. Mukange B., Bantidi M., Zana L., Wafula M., Zana Nd., (2015). The isoseismal map and their implication to underlining ground degree of heterogeneity (Kabalo quake's case, September 11, 1992, magnitude 6.7, Upemba Rift). *Greener Journal of Geology and Earth Sciences*, vol. 3 (2), pp 030-042.

8. Mukange B., (2016). *Conception d'un modèle physique pour la caractérisation et la surveillance de l'activité sismique et son implication géologique (Cas de la République Démocratique du Congo).* Thèse de Doctorat : Université de Kinshasa, Faculté des Sciences. Département de Physique.

9. Mukange B., (2021a). Design of a unified scale for the characterization of seismic activity. International Journal of Innovative Science and Research Technology, Volume 6, Issue 7 , July– 2021, pp.1407-1422. www.ijisrt.com

10. Mukange B., (2021b). Application of the unified scale to the characterization of seismic activity of the Democratic Republic of Congo and its surroundings (comparative study for Africa, Indonesia and the Pacific coast of Central America). International Journal of Innovative Science and Research Technology, Volume 6, Issue 7, July– 2021, pp.1516-1555.

11. Mukange B., (2023a). Characterization of the volcano-seismic activity around Nyiragongo volcano and location of its crater by means of unified scale. *Greener Journal of Geology and Earth Sciences*, 5(1) December 2023: 28-51. http//gjournals.org/GJGES.

12. Mukange B., (2023c). Highlighting the fine structure of the seismic zones of the western branch of the east african rift system using the unified characterization scale and its geological implication. *Greener Journal of Geology and Earth Sciences*, 5(1) December 2023: 76-108. http//gjournals.org/GJGES.

13. Ongendangenda A., (2020). Volcanologie de la chaîne des Virunga. Paris: L'Harmattan.

14. Wafula M., D. Atiamutu et M. Ciraba, (1999). Activité séismique dans les Virunga (Rép.Dém. Congo) liée aux éruptions du Nyiragongo et Nyamuragira, deNovembre 1994 à Décembre 1996. *Mus. roy. Afr. centr. Tervuren Belg., Dépt.Géol. Min. Rapp. Ann. 1997 & 1998*, pp. 309 - 319.

15. Wafula M.D., Kasereka M., Rusangiza K., Kuvuke K., Mukambilwa K., Ciraba M. &Bagalwa M., (2009). The Nyamulagira Volcanic Eruption on November 27, 2006,Virunga Region, D.R. Congo. *Cahiers du CERUKI, Numéro Spécial CRSN-Lwiro(2009)*, pp. 108 - 115.

16. Wafula M.D, Zana A. Kasereka M. and Hamaguchi H., (2011a). The Nyiragongo volcano: A case study for the Mitigation of Hazards on an African Rift Volcano, Virungaregion, Western African Rift Valley, 32 pp.

17. Disponible sur: *http://iugg georisk.org/presentations*

18. Wafula M., (2011b). *Etude Géophysique de l'Activité Volcano-Séismique de la Région des Virunga, Branche Occidentale du Système des Rifts Est-Africains et son Implication dans la Prédiction des Eruptions Volcaniques*. Thèse de Doctorat : Université de Kinshasa, Faculté des Sciences.

19. Zana N, (1977). *The Seismicity of the Western Rift Valley of Africa and related problems*. Doctorat Theses, Tôhoku University. 189 pp.

20. Zana N. and K. Tanaka, (1981). Focal mechanism of major earthquakes in the WesternRift Valley of Africa,*Tôhoku Geophys. Journ. (Sci. Rep. Tôhoku Univ. Ser. 5),* Vol.28, Nos 3-4, pp: 119 - 129.

Cite this Article: Mukange, BA; Kuzituka, T; Zana, NA; Tondozi, KF (2023). Characterization of the Volcano-Seismic Activity around Nyamulagira Volcano and the Location of its Crater by Means of Unified Scale*. Greener Journal of Geology and Earth Sciences*, 5(1): 52-75.